

COORDINATED ASSEMBLY OF BRIGHTEST CLUSTER GALAXIES

MENG GU¹, CHARLIE CONROY¹ AND GABRIEL BRAMMER²*Submitted to ApJL*

ABSTRACT

Brightest Cluster Galaxies (BCGs) in massive dark matter halos are shaped by complex merging processes. We present a detailed stellar population analysis in the central region of Abell 3827 at $z \sim 0.1$, including five-nucleus galaxies involved in a BCG assembly. Based on deep spectroscopy from Multi Unit Spectroscopic Explorer (MUSE), we fit the optical spectra of 13 early-type galaxies (ETGs) in the central 70 kpc of the cluster. The stellar populations in the central $R = 1$ kpc of these ETGs are old (6–10 Gyr). Their $[\text{Fe}/\text{H}]$ increases with σ_* and stellar mass. More importantly, $[\alpha/\text{Fe}]$ of galaxies close to the cluster center do not seem to depend on σ_* or stellar mass, indicating that the cluster center shapes the $[\alpha/\text{Fe}]$ – σ_* and $[\alpha/\text{Fe}]$ – M_* relations differently than other environments where $[\alpha/\text{Fe}]$ is observed to increase with increasing σ_* or M_* . Our results reveal the coordinated assembly of BCGs: their building blocks are different from the general low mass populations by their high $[\alpha/\text{Fe}]$. Massive galaxies thus grow by accreting preferentially high $[\alpha/\text{Fe}]$ systems. The radial profiles also bear the imprint of the coordinated assembly. Their declining $[\text{Fe}/\text{H}]$ and flat $[\alpha/\text{Fe}]$ radial profiles confirm that the accreted systems have low metallicity and high $[\alpha/\text{Fe}]$ stellar contents.

Keywords: galaxies: clusters: individual (Abell 3827) — galaxies: stellar content — galaxies: evolution

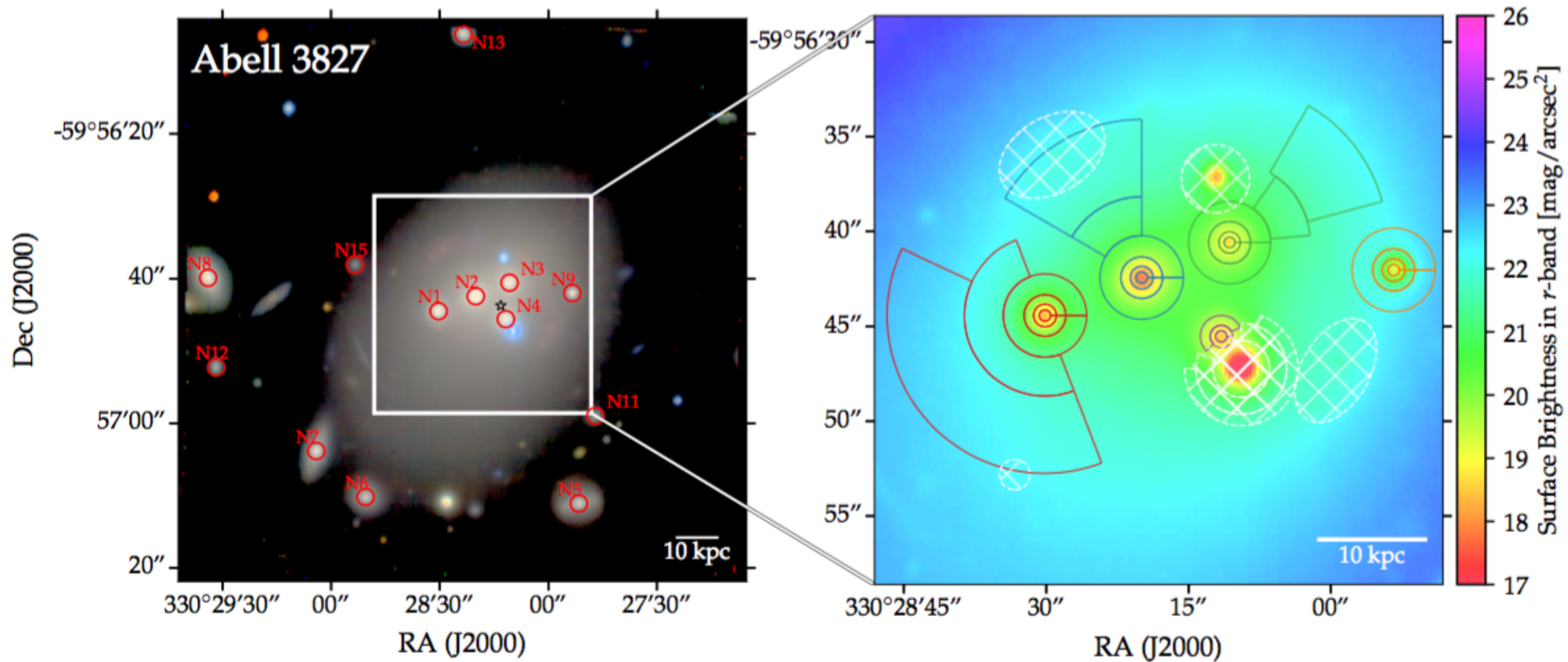
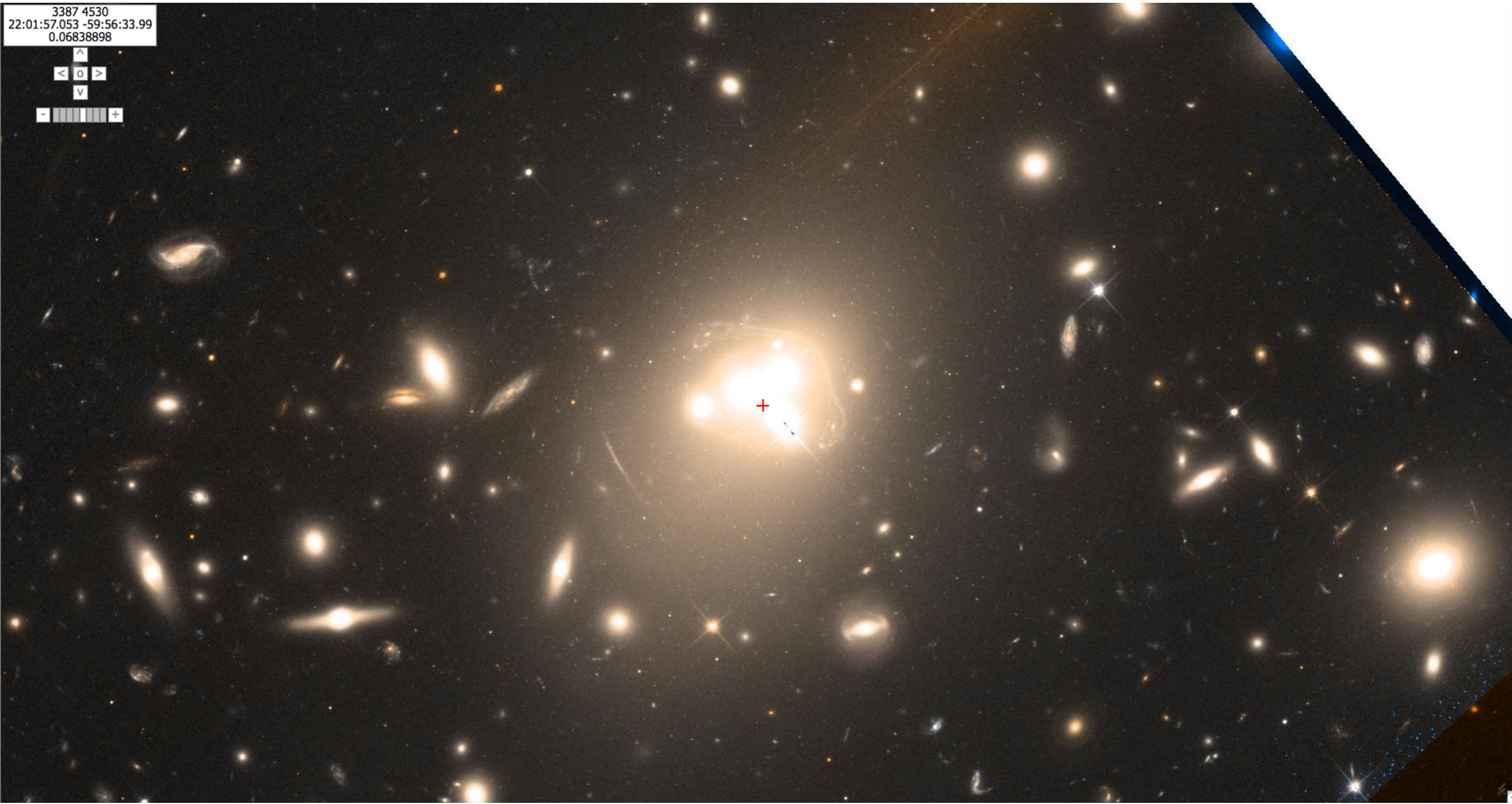
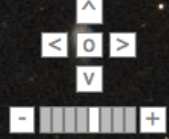
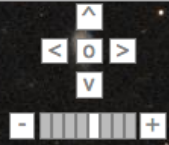


Figure 1. Left panel: Overview of the locations of ETGs studied in this paper on a SDSS-*r**i**z* composite image derived from the MUSE datacube. Red circles enclose $R = 2$ kpc. Right panel: Zoomed-in SDSS-*r* band surface brightness map derived from the MUSE datacube. Solid lines enclose stacked regions for stellar population profiles. White hatched regions highlight masked out spaxels.

3387 4530
22:01:57.053 -59:56:33.99
0.06838898



3387 4530
22:01:57.053 -59:56:33.99
0.06838898



To model galaxies spectra we use the absorption line fitter (`alf`, [Conroy & van Dokkum 2012](#); [Conroy et al. 2014, 2018](#)). `alf` enables stellar population modeling of the full spectrum for stellar ages > 1 Gyr and for metallicities from ~ -2.0 to $+0.25$. Parameter space is explored using a Markov Chain Monte Carlo algorithm (`emcee`, [Foreman-Mackey et al. 2013](#)). `alf` adopts the MIST stellar isochrones ([Choi et al. 2016](#)) and uses a new spectral library ([Villaume et al. 2017](#)) that includes continuous wavelength coverage from $0.35 - 2.4 \mu m$ over a wide range in metallicity, which taken from new IRTF NIR spectra for stars in the MILES optical spectral library ([Sánchez-Blázquez et al. 2006](#)). Theoretical elemental response functions were computed with the ATLAS and SYNTH programs ([Kurucz 1970, 1993](#)). They tabulate the effect on the spectrum of enhancing each of the individual elements. With `alf` in “full” mode we fit for parameters including a two burst star formation history, the redshift, velocity dispersion, overall metallicity, 18 individual element abundances, several IMF parameters ([Conroy et al. 2018](#)). Throughout this paper, we use `alf` with the IMF fixed to the [Kroupa \(2001\)](#) form. We use flat priors within these ranges: $-10^3 - 10^5$ km/s for recession velocity, $100 - 1000$ km/s for velocity dispersion, $1.0 - 14$ Gyr for age and $-1.8 - +0.3$ for metallicities. For each spectrum we fit a continuum in the form of a polynomial to the ratio between model and data. The order of polynomial is $(\lambda_{max} - \lambda_{min})/100 \text{ \AA}$. During each likelihood call the polynomial divided input spectrum and model are matched. The continuum normalization occurs in three separate wavelength intervals, $4300 - 5080 \text{ \AA}$, $5080 - 5700 \text{ \AA}$ and $5700 - 6700 \text{ \AA}$.

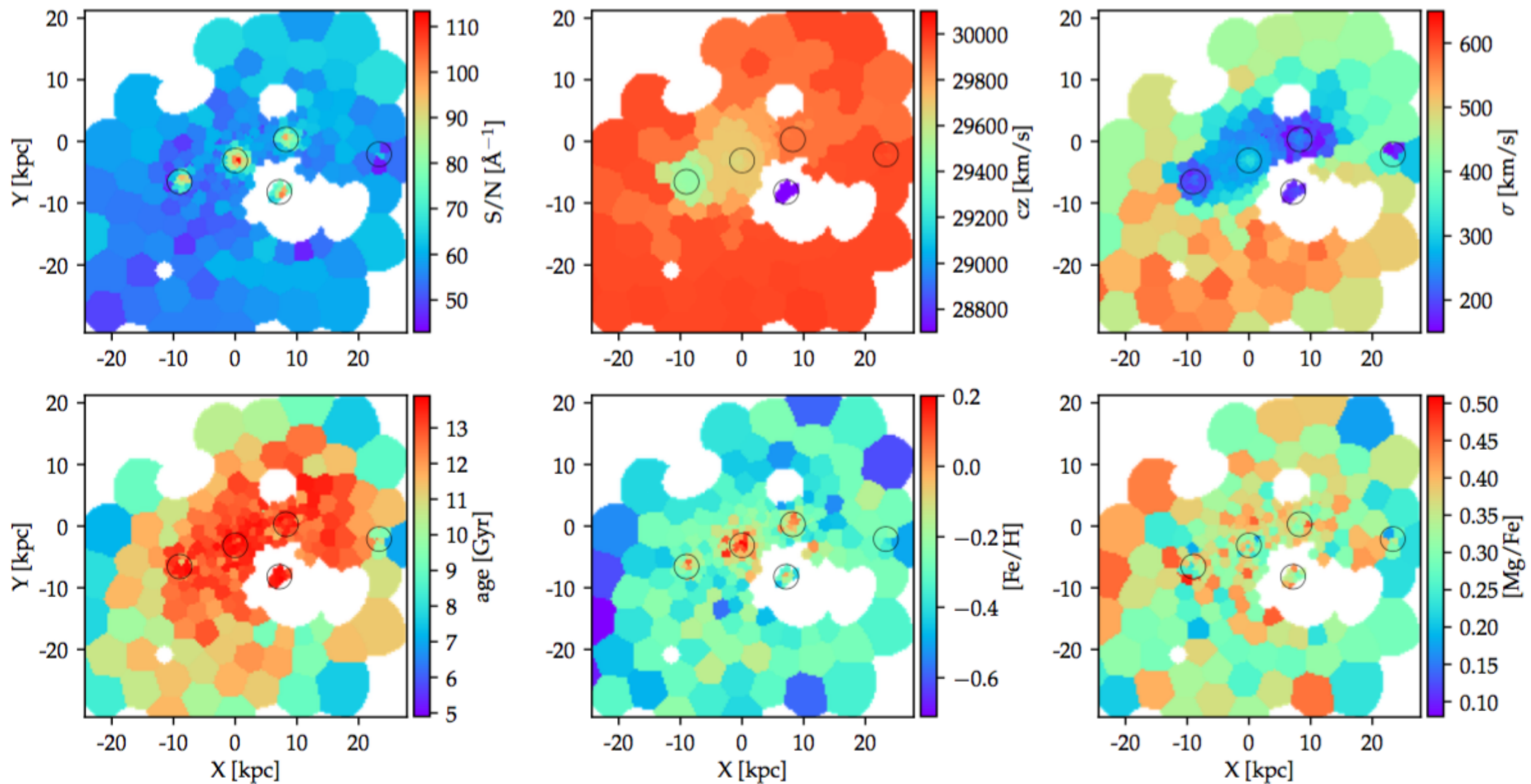


Figure 2. From top left to bottom right: Spatial distribution of the mean S/N per bin in observed frame 4500–5000 Å, recession velocity cz , velocity dispersions σ_* , stellar ages, $[\text{Fe}/\text{H}]$ and $[\text{Mg}/\text{Fe}]$. Black circles enclose $R = 2$ kpc regions of N1–N4 and N9. The typical errors of $\log(\text{age}/\text{Gyr})$, $[\text{Fe}/\text{H}]$ and $[\text{Mg}/\text{Fe}]$ are ≈ 0.03 dex in bins with $S/N > 100 \text{Å}^{-1}$. In regions where σ_* is large, the errors ~ 0.1 dex in bins with $S/N \approx 50 \text{Å}^{-1}$.

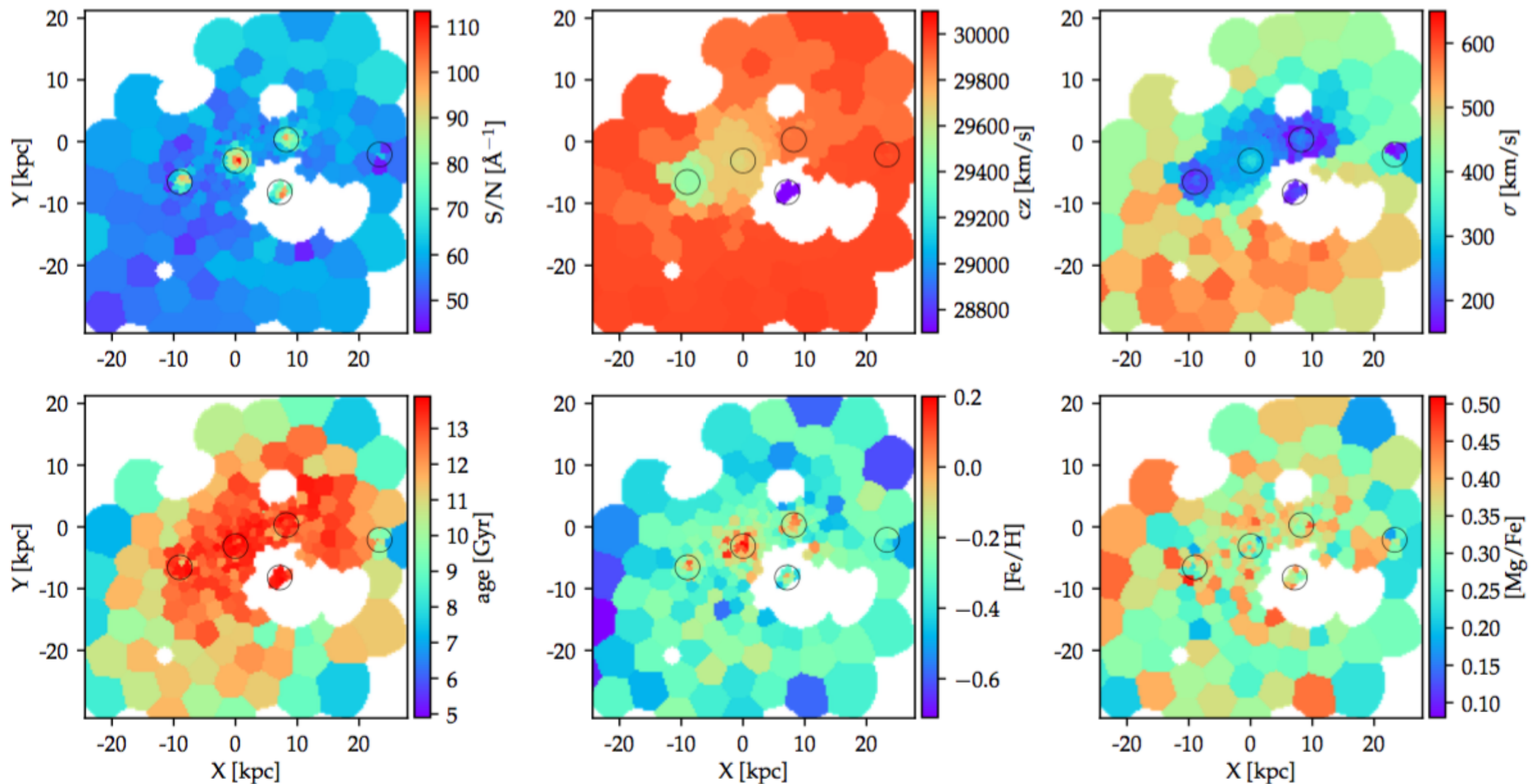


Figure 2. From top left to bottom right: Spatial distribution of the mean S/N per bin in observed frame 4500–5000 Å, recession velocity cz , velocity dispersions σ_* , stellar age, $[\text{Fe}/\text{H}]$ and $[\text{Mg}/\text{Fe}]$. Black circles enclose $R = 2$ kpc regions of N1, N4 and N9. The typical errors of $\log(\text{age}/\text{Gyr})$, $[\text{Fe}/\text{H}]$ and $[\text{Mg}/\text{Fe}]$ are ≈ 0.03 , ≈ 0.03 and ≈ 0.03 , respectively. The typical errors of cz and σ_* are ≈ 100 km/s and ≈ 100 km/s, respectively. The typical errors of S/N are $\approx 50 \text{Å}^{-1}$.

• From the spatial distribution in the central region of the cluster, the stellar populations in the diffuse stellar light of Abell 3827 are generally old and α -enhanced.

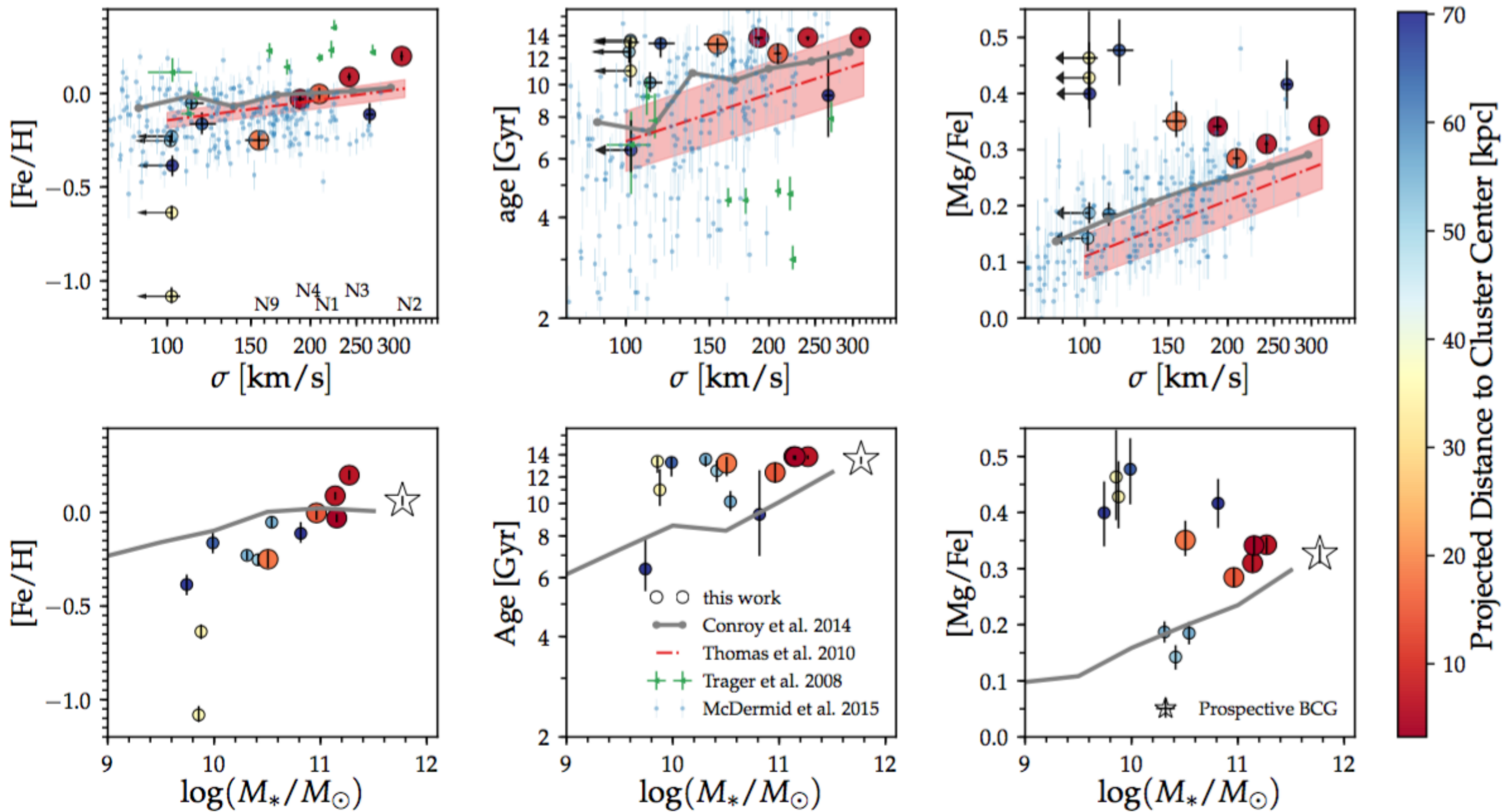
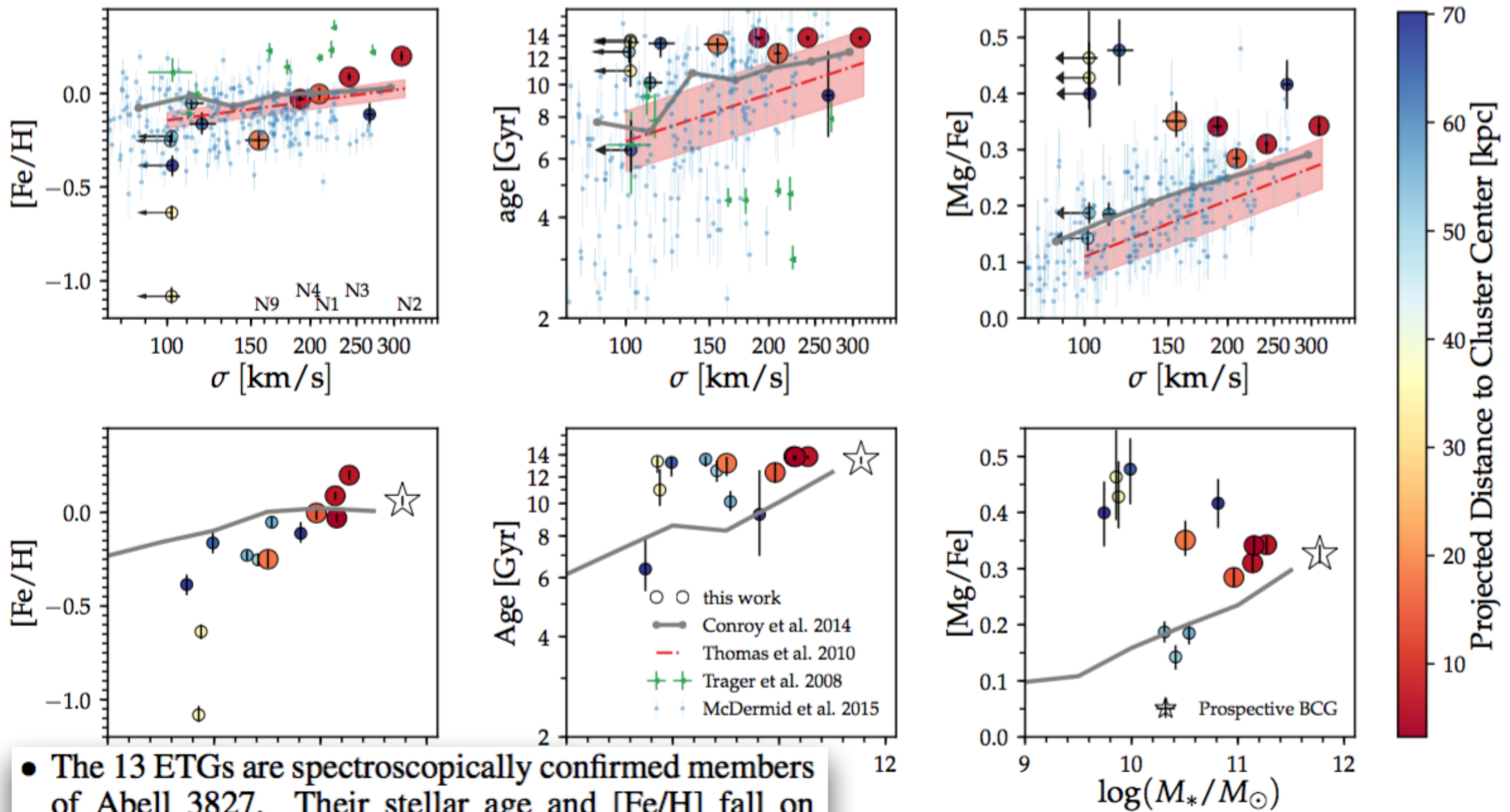


Figure 3. Top: Relationships between σ_* and stellar population parameters: [Fe/H], stellar ages and [Mg/Fe]. Bottom: Relationships between stellar mass measured within $R = 5$ kpc and stellar population parameters measured within $R = 1$ kpc. Colors indicate the projected distance from the center of galaxies to the mass center of the cluster. 13 ETGs in our sample are compared to a large sample of morphologically selected SDSS ETGs in [Thomas et al. \(2005\)](#) (red dash-dotted line), ETGs in ATLAS^{3D} by [McDermid et al. \(2015\)](#) (blue circles), 12 ETGs in the Coma cluster by [Trager et al. \(2008\)](#) (green triangles) and updated results from stacked SDSS ETGs that are binned in σ_* and stellar mass ([Conroy et al. 2014](#)).



- The 13 ETGs are spectroscopically confirmed members of Abell 3827. Their stellar age and [Fe/H] fall on empirical trends that galaxies with higher σ_* or stellar mass are older and more metal rich. However, ETGs within 40 kpc from the cluster center show higher [Mg/Fe] compared to the [Mg/Fe]- σ_* and [Mg/Fe]- M_* relations in the field.

stellar ages and [Mg/Fe]. Bottom: Relationships between stellar mass and [Mg/Fe]. Colors indicate the projected distance from the center of galaxies to the center of morphologically selected SDSS ETGs in Thomas et al. (2005) (red circles) and in the Coma cluster by Trager et al. (2008) (green triangles) and updated by Conroy et al. (2014).

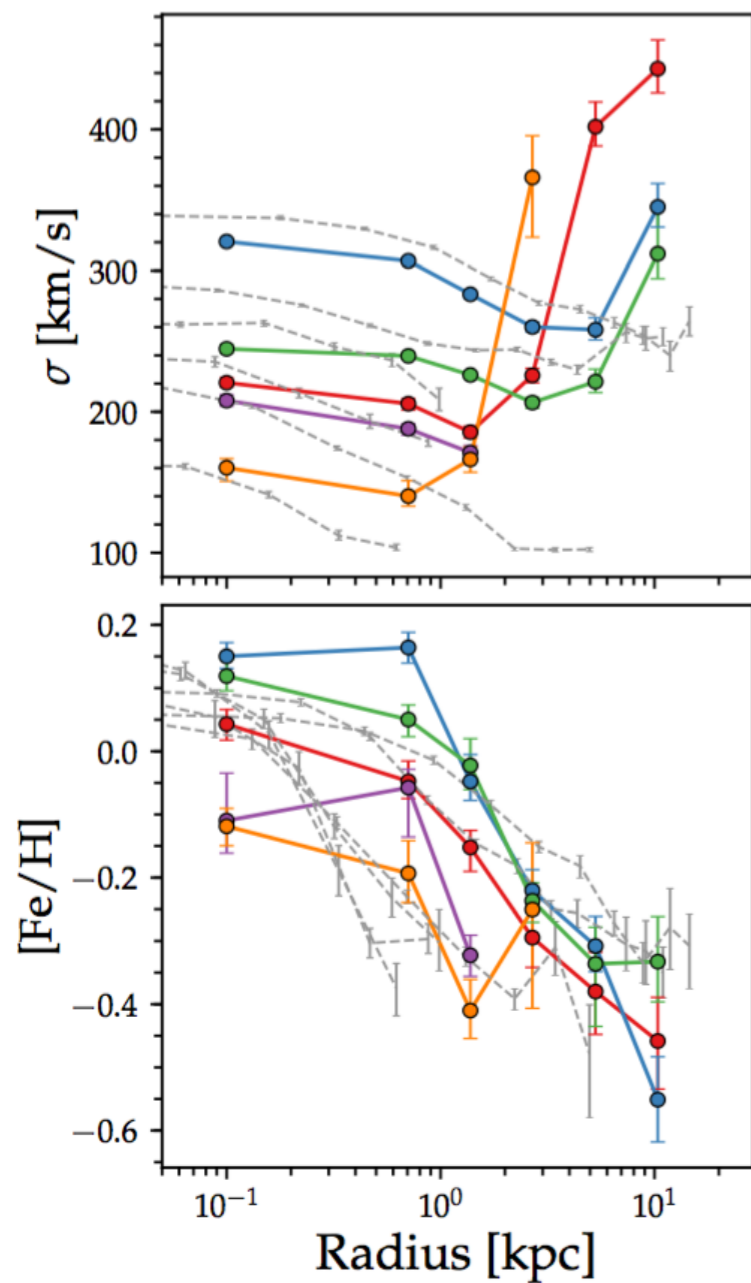


Figure 4. Radial profiles of stellar population parameters. From top right to bottom right: stellar velocity dispersions σ_* , stellar ages, $[\text{Fe}/\text{H}]$ and $[\text{Mg}/\text{Fe}]$ as functions of distance to the center of five galaxies that are closest to the cluster center. Gray dashed lines represent the radial profiles of six ETGs in van Dokkum et al. (2017a).

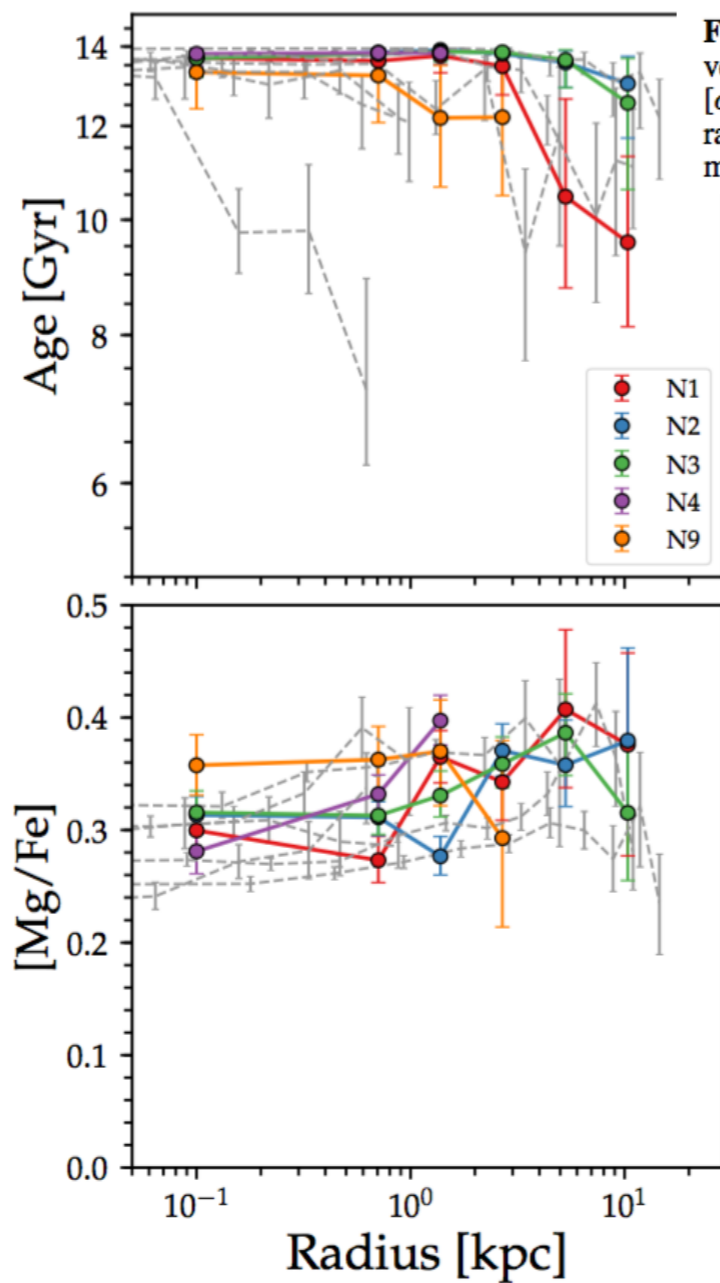
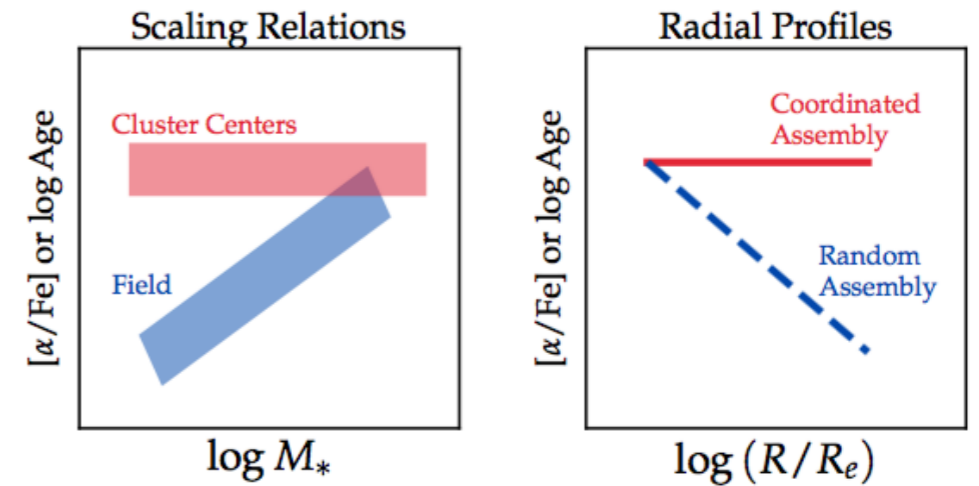


Figure 5. Schematic diagrams for scaling relations of $[\alpha/\text{Fe}]$ or $\log(\text{age})$ versus stellar mass in different environments (left), and the radial profile of $[\alpha/\text{Fe}]$ or $\log(\text{age})$ a massive ETG would build up (right) if it accreted systems randomly in all environments (blue), or coordinately from a sample of low mass galaxies that are quenched early on by the dense environments (red).

- We show the radial profiles of σ_* , stellar age, $[\text{Fe}/\text{H}]$ and $[\text{Mg}/\text{Fe}]$ that are consistent with previous studies. The flat stellar age and $[\text{Mg}/\text{Fe}]$ profiles confirm the coordinated assembly picture.
- Our results highlight the effect of “environmental quenching”, and reveal the coordinated assembly of BCGs: the building blocks of the prospective BCG in Abell 3827 are distinct from the general low mass systems by high $[\alpha/\text{Fe}]$ due to early quenching by the dense environment.

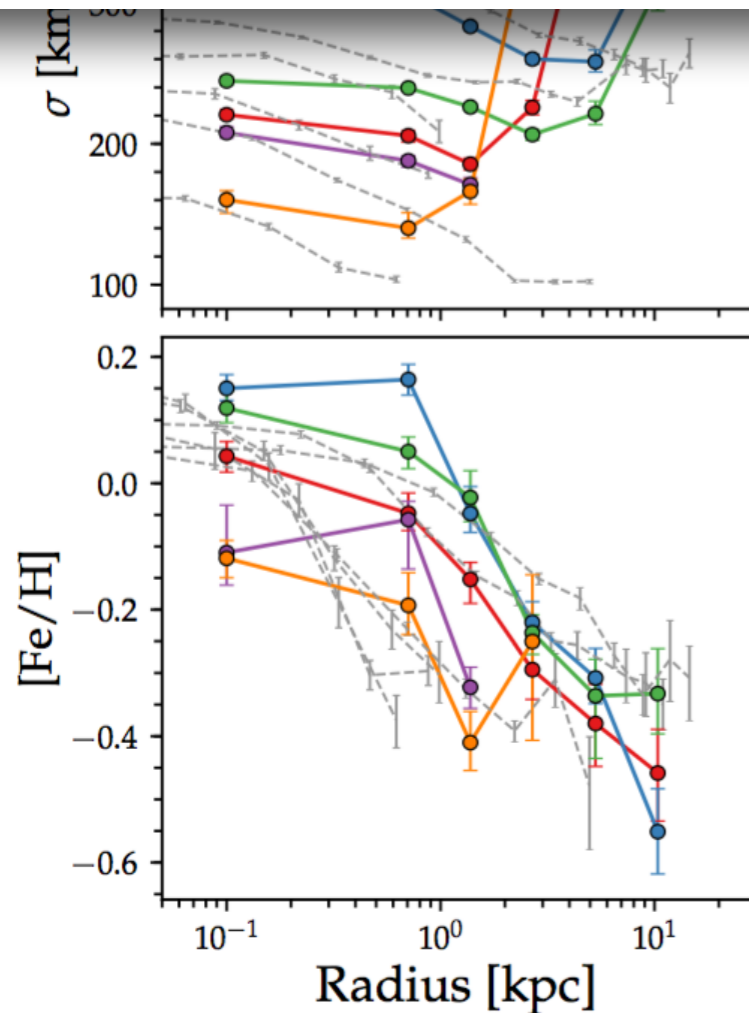


Figure 4. Radial profiles of stellar population parameters. From top right to bottom right: stellar velocity dispersions σ_* , stellar ages, $[\text{Fe}/\text{H}]$ and $[\text{Mg}/\text{Fe}]$ as functions of distance to the center of five galaxies that are closest to the cluster center. Gray dashed lines represent the radial profiles of six ETGs in [van Dokkum et al. \(2017a\)](#).

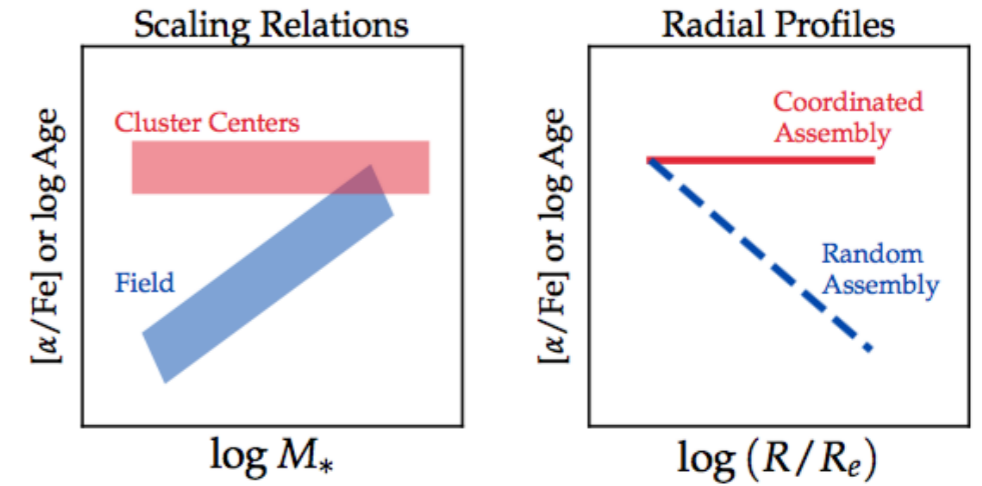


Figure 5. Schematic diagrams for scaling relations of $[\alpha/\text{Fe}]$ or $\log(\text{age})$ versus stellar mass in different environments (left), and the radial profile of $[\alpha/\text{Fe}]$ or $\log(\text{age})$ a massive ETG would build up (right) if it accreted systems randomly in all environments (blue), or coordinately from a sample of low mass galaxies that are quenched early on by the dense environments (red).

The coordinated assembly picture can be described by the schematic diagrams in Figure 5: the building blocks of BCGs are low mass galaxies in a special environment—cluster centers. They follow a relatively flat relation between $[\alpha/\text{Fe}]$ or stellar age and stellar mass (red box), which are distinct from the relations followed by galaxies in the fields (blue box). The right panel of Figure 5 shows the expected radial profiles of the massive ETGs: As the low mass systems in the cluster center accrete onto the outskirts of massive ETGs, the coordinated assembly produces flat radial profiles of stellar age and $[\alpha/\text{Fe}]$ (red), whereas if the accreted systems are random draws from the low mass galaxy sample in all environments the profiles of stellar age and $[\alpha/\text{Fe}]$ would decline with radius.